Exploration of Turbulence Driven Deflagration to Detonation of Fast Flames

Jessica Chambers, Kareem Ahmed
Propulsion and Energy Research Laboratory,
Center for Advanced Turbomachinery & Energy Research,
University of Central Florida
Orlando, FL, USA

Alexei Poludnenko
Department of Aerospace Engineering
Texas A&M University, College Station, TX, USA

1 Introduction

Pressure gain combustion (PGC) is mainly characterized by a stagnation pressure rise in a system. Detonation is a form of PGC that exploits the pressure rise to augment high flow momentum. There is significant interest in this combustion mode as it has high thermodynamic efficiencies and thrust capabilities, making it desirable to enhance the performance of current and next generation propulsion technologies [1]. Predicting and controlling the onset of detonation is a serious challenge as the conditions for detonation have been experimentally uncertain. To generate a detonation wave, the deflagration-to-detonation transition (DDT) process must occur. Traditionally, a DDT process is studied experimentally in semiconfined channels [2, 3], in which the DDT process begins with the ignition of a flame kernel and expansion towards the open end, consuming the reactants ahead. Conventionally, flow obstacles are used to generate turbulence within the flame and induce rapid flame acceleration [4]. Compression waves are generated ahead of the flame and strengthen to form shock waves. As the flame accelerates and approaches the shock, shock reflections create local hot spot explosion centers [5, 6]. This region ahead of the flame becomes highly reactive, and finally, a detonation wave is spontaneously generated. Although this has been the general process of DDT, recent investigations into the mechanisms that drive DDT has been computationally simulated [7]. The key driving mechanisms of the DDT process have not been entirely characterized. In unconfined DDT, it is not fully identified how DDT can successfully develop into a detonation. Understanding of this phenomenon can apply to a variety of systems ranging from open-air fuel-vapor-cloud explosions in industrial settings to fuel-air explosive munitions to astrophysical objects such as supernovae explosions. Only hypothesized in computational simulations, with high enough turbulence levels and flame acceleration, the self-propagating flame produces violent flame collisions and a highly compressed region ahead of the flame front. There is a need to explore these conditions for the characterization of turbulent induced DDT.

The fundamental mechanism for achieving detonation is turbulent flame acceleration from deflagration-to-detonation. The process involves generation of high flow turbulence intensities and length scales for effective flame acceleration and propagation [8]. Turbulence generation is critical for flame acceleration and propagation. To achieve DDT, the flame is accelerated by turbulence induction. Conventionally, flame turbulence is achieved using in-flow solid obstacles. The obstacles produce turbulence which increases flame burning rates and propagation velocities by distorting and expanding flame surface area. Higher turbulence enhances rapid transport between reactants and products which increase burning rates and consequently higher turbulent burning velocities. Flame acceleration to DDT undergoes various distinct stages of evolution, which are governed by the mixture characteristics. The flame experiences various stages of propagation velocities such as the sonic velocity – the speed of sound in the reactant mixture (at STP conditions), the isobaric sonic velocity –the speed of sound in the product region, and the Chapman-Jougeut (CJ) detonation velocity. A flame at low subsonic velocity is characterized as a slow deflagration until it surpasses the sonic velocity. This is when weak compression waves begin to form ahead of the flame, in the fast deflagration regime. Here, the flame travels at several hundreds of meters per second. As the flame evolves to higher speeds, a thick compressed region of reactants form immediately ahead of the flame front. Once the flame surpasses the isobaric sonic velocity, it transitions into the quasi-detonation mode where it couples closely with the compressed region and the leading shock on a small length scale. The flame velocity rapidly accelerates to the CJ detonation velocity, where it is classified as a fully matured detonation wave. These modes of DDT flames are explored in the results.

During the fast deflagration stage, the formation of the compressed reactants region within close proximity of the flame front is a key characteristic of the conditions that lead to the transition to detonation. This region is a consequence of the initial reactant conditions, i.e., flame turbulence levels, and flame propagation velocity. Numerical simulations capture a pressure buildup at the flame front which interacts with the augmented flame, initiating a runaway mechanism that leads to the transition to detonation [9, 10]. The assertion presented by these simulations relates the turbulent flame speed, S_T, representing the rate of reactant consumption, to the CJ deflagration velocity, S_{CJ}, which is the ratio of the sonic velocity to the density ratio across the flame. Once the turbulent flame speed surpasses the CJ deflagration velocity, DDT will occur. This condition is also related to the flame turbulence levels and length scales. All of these conditions that guarantee a DDT occurrence have not been classified in previous experimental work. To understand the specific boundary conditions for the flame of interest, the flame evolution, reactant field, and compressed region are thoroughly investigated in this study.

An in-depth study is conducted to provide observations and analysis of fast hydrogen-air flames to help predict the conditions for the onset of DDT. Almost all instances of DDT have been observed to have a similar basic mechanism. However, the prediction and control of the occurrence of DDT require further exploration. Advanced laser optical diagnostics (simultaneous PIV and chemiluminescence), pressure, and temperature measurements are leveraged to explore the flow field and capture the critical flame behavior that will lay the groundwork for a further focused exploration of the critical conditions that guarantee a DDT occurrence.

2 Experimental Setup and Diagnostics

The flame interaction with turbulence is explored to identify the key mechanisms for various turbulent flame regimes. An optically accessible turbulent deflagration-to-detonation facility is used for the research. The experimental facility, shown in Figure 1, is a semi-confined square channel with height and width of 45 mm x 45 mm. The center 6” test section has optical access to the flow on three sides using 1” thick fused silica glass to allow for non-invasive flow laser diagnostics. The facility geometry is similar to that of the DNS simulations by Poludnenko and Oran, with the principal difference being in the spanwise boundaries, which are periodic in DNS calculations [9]. The facility is configurable with various geometrical configurations to induce several modes of turbulence generation to probe the turbulent flame dynamics from low flame turbulence to detonating turbulent flames in the distributed broken reaction regime. The turbulator consists of 6 perforated plates in series, as shown in Figure 2. This specific geometric configuration easily provides a survey of all the regimes of interest, in particular, the conditions for turbulence driven DDT and was the result of extensive experimental testing to achieve the desired flame-turbulence conditions.

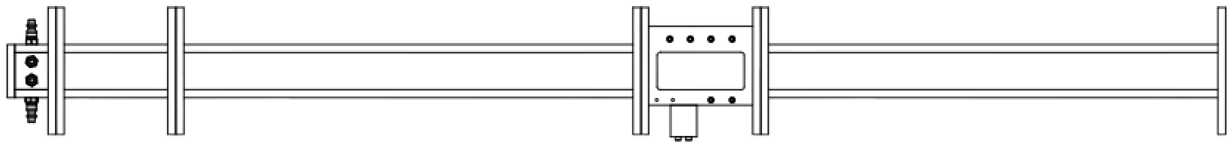

Figure 1: Semi-confined channel with viewing window

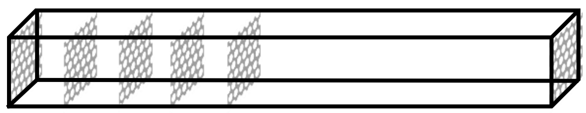

Figure 2: Turbulator configuration

A fuel-air delivery system is regulated to change fuel-air concentrations using a series of pressure regulators and flowmeters. A compressed air line and hydrogen fuel tank are regulated down to a low pressure to control the flow velocity, and Dwyer VFA-4 flowmeters are used to control the fuel concentration. System timing is controlled using a BNC Model 575 Pulse/Delay Generator. Once the flow meters are set, and the chamber is filled with the reactant mixture, the pulse generator sends a TTL signal to an Omega SSRL240DC10 relay which powers the fast responding solenoid valve to exhaust the flow from the lines. The spark plug is then triggered by the timing box 2 seconds later, powered by an ACCEL Super Coil 140001 and Tektronix PWS4205 power supply. With the same timing, the camera is sent a signal, and the reactant mixture ignited so that the optical diagnostics in place capture the Schlieren images. High speed Schlieren is used to observe overall flame and shock behavior after the high turbulence induction in the obstacle-filled facility. The images are captured using Photron Fastcam SAZ cameras recording at a rate of 75 kHz.

Simultaneous high-speed particle image velocimetry (PIV) and OH* chemiluminescence along with dynamic pressure measurements (PCB 113B26, Range: 500 psi, sensitivity: 10 mV/psi, resonant Frequency: 1 MHz) are implemented to characterize the flame-flow characteristics throughout the interaction. The pressure transducer measurements were validated relative to the shock strength from gas dynamics equations. The main flow is seeded with aluminum oxide particles distributed throughout the reactant field and illuminated by a 20 kHz, 20 mj, LDP Dual Laser. The Photron Fastcam SAZ camera with 1,024 x 1,024 pixels spatial resolution and 16-bit range with a 50 mm Nikon lens at f # of 1.2 records the seeded flame interaction at 40,000 fps using frame straddling mode. All images are acquired using Photron Fastcam computer software.

3 Results

The research characterizes the compressibility of highly turbulent fast flames to understand the mechanisms for the turbulent deflagration-to-detonation phenomenon. Generally, the propagation of deflagration-to-detonation flames is classified in various regimes as shown in Figure 3. There are four main regimes: deflagrations, fast deflagrations (fast flames), quasi-detonation, and detonation. The turbulator section of the facility was tuned to allow the ability to sweep across these various regimes through the control of the equivalence ratio at a fixed spatial domain, specifically, the optical access test section domain. The figure shows the flame speeds along with Schlieren images of the classes of flames that are explored. As shown in Figure 3a, fast deflagration flames that surpass the sonic velocity of the gas, begin to experience gas compressibility ahead of the flame. This compressibility region couples with the flame as the flame reaches the isobaric sonic velocity, i.e., the isobaric products speed of sound. At this condition, Fig. 3b, it is expected that the turbulence driven DDT will occur. Beyond this stage, the flame, compressible region, and shock couple together as shown in Figure 3c. They further combine rapidly in a quasi-detonation form, Fig. 3d. The flame continues to accelerate in the quasi-detonation regime reaching the Chapman–Jouguet detonation speed. The critical stage for turbulence-driven DDT to occur is the condition where the flame is in the fast deflagration regime, below the isobaric sonic velocity. Beyond that stage, the flame is expected to rapidly accelerate through the quasi-detonation to detonation. Therefore, the research focused on characterizing the critical flame condition that defines the turbulent mode of DDT, Fig 3b.

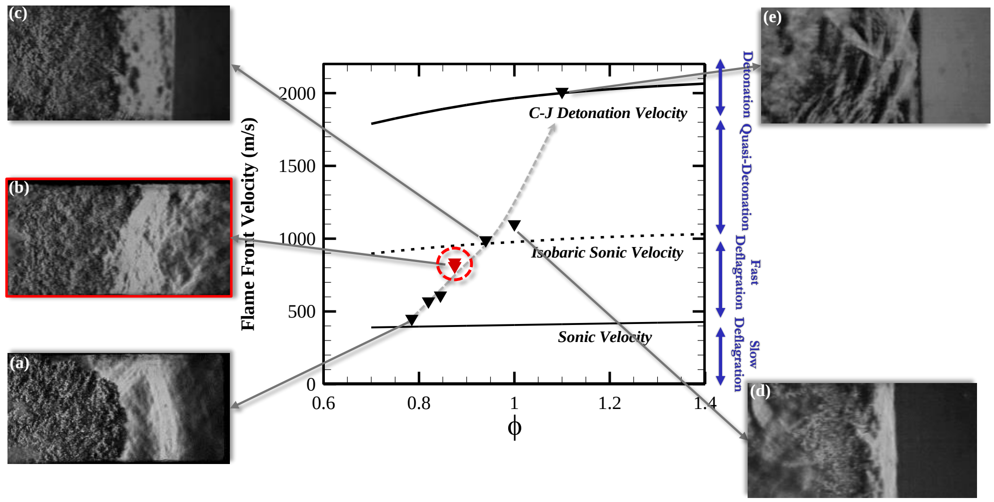

Figure 3. Propagation regimes of deflagration-to-detonation flames

Exploring the turbulence driven DDT process, the interaction of the turbulent fast flame with the compressible region is presented in Figure 4. This flame is at the condition of Fig. 3b. The images show the temporal evolution of the flame-compressibility region within the optical domain. The turbulent fast-flame enters the domain with a broad compressible region ahead. As the flame accelerates, it results in self-compression of the reactant gas ahead. Localized lateral flame collisions occur amplifying the compression region within close proximity of the flame. This leads to an abrupt acceleration and a transition to a quasi-detonation

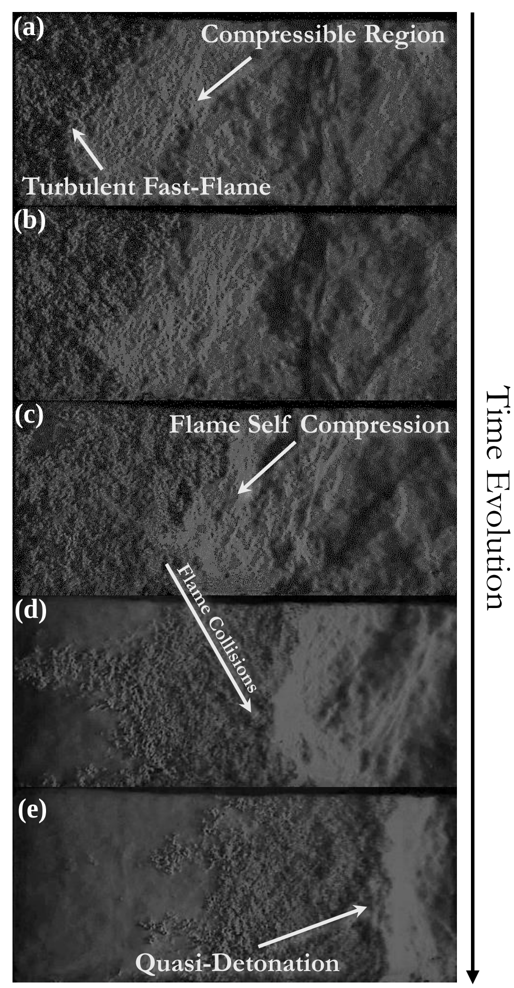

Figure 4. Temporal evolution of turbulent Deflagration-to-detonation transition

mode. In that mode, the flame and the compressible region straighten, similar to Fig. 3c. The flame-compressible region progress to catch up to the leading shock forming the coupling shown in Fig. 3d.

The general hypothesis for turbulence-driven deflagration-to-detonation is that the turbulent flame speed, S_T, would be on the order of the Chapman–Jouguet deflagration speed, S_{CJ} [10]. The investigation examined the local property conditions that led to the turbulent flame transition for the case shown in Figure 4. The properties have been computed for the un-burnt compressible region and the burnt region based on the locally measured conditions. These properties are tabulated in Table 1. The pressure and temperature are the measured values within the compressible region, immediately ahead of the flame. The temperature is quantified using isentropic equations from the measured initial temperature, pressure, and velocity. Using these conditions, the speed of sound for the reactants and products could be evaluated through thermodynamic equilibrium reaction computation. The Chapman–Jouguet deflagration flame speed is assessed through the speed of sound relative to the density ratio of reactants to products, as shown in Equation 1. The Chapman–Jouguet flame speeds based on the fuel and the products along with the laminar flame speed are also included in the table.

Property	Value
T (K)	627
P (bar)	7.02
$S_{CJ,f}$ (m/s)	168.2
$S_{CJ,p}$ (m/s)	292.4
S_L (m/s)	4.68

Table 1: Local flame-compressible region properties

$$S_{CJ} = \frac{c_s}{\alpha}, \quad where \quad \alpha = \frac{\rho_{reactants}}{\rho_{products}} \; and \; c_S = \sqrt{\gamma RT} \tag{1}$$

The local turbulent flame speed, S_T, is quantified using simultaneous measurements of OH* and PIV. The overlap of the flame on the flowfield is shown in Figure 5. Since the flame front is propagating in one direction and the reactant flow is traveling at a near constant bulk velocity, S_T could be evaluated from the simultaneous flame-flow measurement. The turbulent flame speed is computed from the relative velocity between the propagating flame velocity and the reactant velocity, i.e., reactants consumption speed. The flame propagation velocity is found to be 763 m/s. The reactants gas ahead of the flame is traveling at an average 377 m/s (105 m/s r.m.s.) within the domain highlighted in the Figure. These velocities result in a S_T = 385±11 m/s. Consequently, the turbulent flame speed is greater than the Chapman–Jouguet deflagration flame speed both in the reactants and product, which classifies the flame within the spontaneous transition regime, i.e., the DDT runaway process has been initiated. This corroborates the previously made conclusion [10] that at $S_T > S_{CJ,p}$ turbulent deflagration-to-detonation is expected to occur.

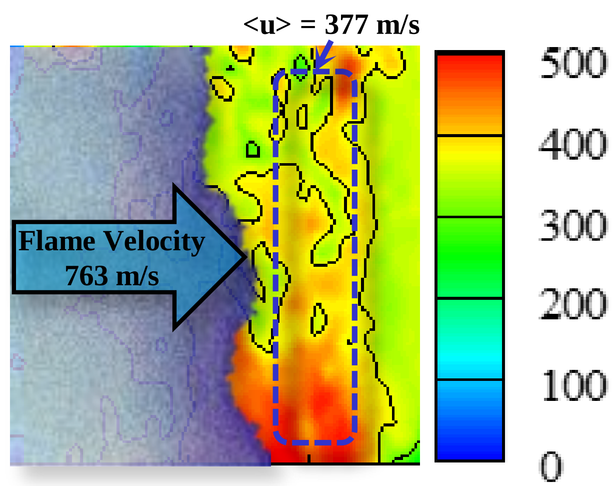

Figure 5. The fast turbulent flame superimposed on the PIV axial velocity field

4 Conclusion

The research explores the local conditions for turbulence-based deflagration-to-detonation transition of fast flames. The experimental investigation explored the classification of various flames from fast flames to detonation flames identifying the main flame characteristics. A turbulent fast flame condition that is on the verge of transitioning to quasi-detonation was examined showing the key characteristics for turbulent flame DDT. The Chapman–Jouguet deflagration flame speed has been evaluated based on the local properties of the reactants and products. Simultaneous measurements of the flame-flow field were used to quantify the turbulent flame speed. The turbulent fast flame was within the spontaneous transition regime and the DDT runaway stage. It is also shown that the turbulent flame speed is on the order of the Chapman–Jouguet flame speed for a transitional deflagration-to-detonation fast flame.

Acknowledgements

The work is sponsored by the Air Force Office of Scientific Research (FA9550-16-1-0403, Program Manager: Dr. Chiping Li) and the American Chemical Society Petroleum Research Fund (54753-DNI9). The authors would like to acknowledge the Donors of the American Chemical Society Petroleum Research Fund for support of this research.

References

[1] Wu, Y., F. Ma, and V. Yang. (2003). System performance and thermodynamic cycle analysis of airbreathing pulse detonation engines. Journal of Propulsion and Power. 19(4): 556.

[2] Ciccarelli, G. and S. Dorofeev. (2008). Flame acceleration and transition to detonation in ducts. Progress in Energy and Combustion Science. 34(4): 499.

[3] Boeck, L. R., et al. "Simultaneous OH-PLIF and schlieren imaging of flame acceleration in an obstacle-laden channel." Proceedings of the Combustion Institute 36.2 (2017): 2807-2814.

[4] Lee, S.-Y., et al. (2004). Deflagration to detonation transition processes by turbulence-generating obstacles in pulse detonation engines. Journal of Propulsion and Power. 20(6): 1026.

[5] Zel'Dovich, Y.B., et al. (1970). On the onset of detonation in a nonuniformly heated gas. Journal of Applied Mechanics and Technical Physics. 11(2): 264.

[6] Oran, E.S. and A.M. Khokhlov. (1999). Deflagrations, hot spots, and the transition to detonation. Philosophical Transactions of the Royal Society of London A: Mathematical, Physical and Engineering Sciences. 357(1764): 3539.

[7] Oran, E.S., V.N. Gamezo, and D.A. Kessler. (2011). Deflagrations, detonations, and the deflagration-to-detonation transition in methane-air mixtures. DTIC Document.

[8] Andrews, G., D. Bradley, and S. Lwakabamba. (1975). Turbulence and turbulent flame propagation—a critical appraisal. Combustion and Flame. 24: 285.

[9] Poludnenko, A.Y. (2015). Pulsating instability and self-acceleration of fast turbulent flames. Physics of Fluids. 27(1): 014106.

[10] Poludnenko, A.Y., T.A. Gardiner, and E.S. Oran. (2011). Spontaneous transition of turbulent flames to detonations in unconfined media. Physical Review Letters. 107(5): 054501.